



MOLECULAR DYNAMICS STUDY ON THE STRUCTURAL, THERMAL AND ENERGETIC PROPERTIES OF GaAs NANOPARTICLES

Mustafa KURBAN *

Department of Electronics and Automation, Ahi Evran University, 40100 Kırşehir, Turkey

ABSTRACT

In this work, the structural and energetic properties of GaAs nanoparticles (NPs) are investigated using the bond order potential (BOP) based on modern classical molecular dynamics (MD) method. All MD simulations are performed by means of LAMMPS (large-scale atomic/molecular massively parallel simulator). Some physical properties such as variation of potential energy depending on temperature, order parameter, coordination number in terms of probability distribution and radial distribution function (RDF) are searched. The heat capacity (C_v) calculation is also performed as depending on temperature using a non-equilibrated molecular dynamics simulation strategy. The tendency of Ga and As atoms inside the core has been observed under temperature increase. As atoms have significant effect on the stability of GaAs NPs. Temperature dependence of these physical properties was obtained. The calculated physical properties are found to be sensitive to temperature.

Keywords: Nanoparticles; Coordination number; Segregation formation; Heat capacity; Molecular dynamics

1. INTRODUCTION

Nanoparticles (NPs) are predicted to have many distinctive properties comparing with their bulk materials. Therefore, NPs have recently attracted strong interest in many applications including energy, electronics, biomedical and optoelectronic industry. They can be classified into different groups based on the type of NPs such as metal, semiconductor, insulator or organic NPs. Among these types, semiconductor NPs have been widely investigated because the materials have been found useful in important applications [1-3]. Considering III–V semiconductors, especially, gallium arsenide (GaAs) is the most important representative due to its use in high-efficiency solar cell [4]. In this regard, GaAs has been subject of intensive research in both experimentally and theoretically to understand the structural, mechanical, thermal and electronic properties and demonstrate a highly efficient properties of this material [5-11].

The properties of materials at nanolevel modify the traditional electronic structures and thus provide new opportunities for the semiconducting industry including optoelectronics, photovoltaic and solar cell applications. For example, the optical properties of GaAs NPs enhance because of the change in energy band gap of GaAs at nanoscale [12]. Recently, the enhanced properties obtained from the changes of size and shape or optical and electrical control of GaAs quantum dots (QDs) have been showed in different studies [13, 14].

A fundamental understanding of physical properties of GaAs material is still in demand at nanolevel. Investigations of GaAs NPs with different composition under heat treatment have been not reported yet. To our knowledge, there is no theoretical studies of GaAs NPs exist in literature. Therefore, the primary scope of this work is to explore some physical properties such as the variation of potential energy depending on temperature and composition, heat capacity (C_v), order parameter (R), coordination number in terms of probability distribution and radial distribution function (RDF) of zinc-blende GaAs spherical-like binary NPs using bond order potential (BOP).

2. THE METHOD OF CALCULATIONS

A modern version of MD simulations with LAMMPS (large-scale atomic/molecular massively parallel simulator) [15, 16] were performed using Ga-As binary analytical BOP [17]. Conventional MD methods, such as Stillinger-Weber (SW) and Tersoff (TR) potentials, cannot give structural properties of systems because they have not been parameterized with the correct physics. For example, crystalline growth is difficult to achieve with TR potentials and defect formation cannot accurately be revealed with SW potentials. In this regards, Ward and co-workers showed that only a BOP approach could adequately predict growth mechanisms [18-20] and can in principle offer a more accurate description of interatomic interactions compared to SW and TR potentials. Unlike the SW and Tersoff-Brenner potentials, BOP is analytically derived from quantum mechanical theories under the condition that the first two levels of the expanded Greens function for the σ and π bond orders are retained. Total of 56 parameters were defined for the BOP. The detail of the physics and parameterization of the Ga-As BOP is given in Ref. [17].

In the simulations, a Nosé Hoover thermostat [21, 22] (in NVT ensemble) is used to control thermal equilibrium of the system. The energetic relaxation is performed at fixed geometry (stable structure). The simulations are carried out starting at 1 K and the temperature of the system is increased by 25 K up to 900 K for Ga-As spherical clusters with different size and composition. At every temperature rise the systems are relaxed for about 0.1 ns. The system is gradually annealed (25 K) without waiting for thermal equilibrium. The initial velocities are determined from Boltzmann distribution at the temperature. The choice of the cut-off generally depends on the potential used. For the BOP an effective cutoff is 14.70 Å since the BOP many body calculations involve neighbors of neighbors of neighbors. The initial views of the Ga₁₇As₁₃, Ga₃₅As₁₉, Ga₅₅As₄₄ and Ga₈₇As₈₀ clusters are shown in Figure 1 [23].

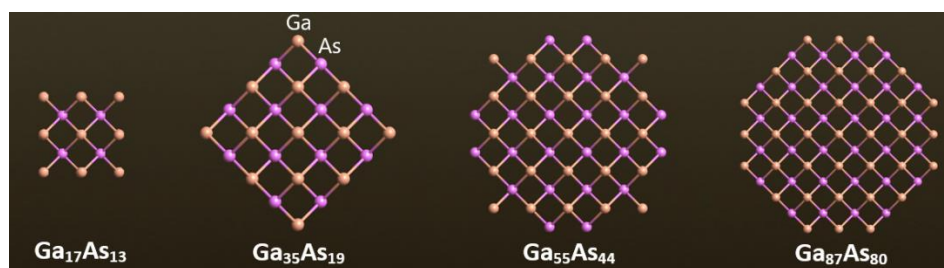


Figure 1. The initial structures of the Ga₁₇As₁₃, Ga₃₅As₁₉, Ga₅₅As₄₄ and Ga₈₇As₈₀ nanoparticles

3. RESULTS AND DISCUSSIONS

MD simulations are performed to demonstrate the segregation formation, size and composition dependence properties of Ga₁₇As₁₃, Ga₃₅As₁₉, Ga₅₅As₄₄ and Ga₈₇As₈₀ NPs. In this regards, I have calculated the variation of potential energy based on temperature and composition, heat capacity (C_v), order parameter (R), coordination number in terms of probability distribution and radial distribution function (RDF) and compared with the available results in the literature.

Figure 2 shows that variation of the potential energy as a function of temperature for Ga₁₇As₁₃, Ga₃₅As₁₉, Ga₅₅As₄₄ and Ga₈₇As₈₀ NPs. Depending on the increment of temperature, the variation of average energy represents rather linear increase, however; a decrease in the per-atom potential energy is noted, as by increasing the size, the surface-to-volume ratio decreases and the structure of the NP also transforms from more amorphous-like to more crystalline-like, and energy approaches the level of bulk energy. The same trend of temperature dependence of potential energy has been observed for the bulk of liquid GaAs system [24].

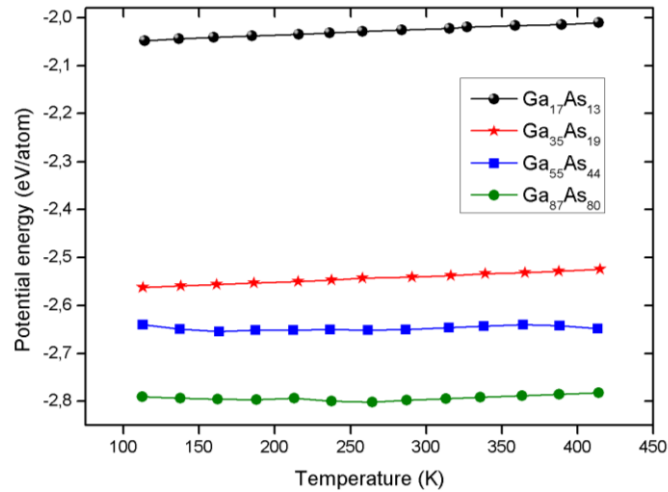


Figure 2. Variation of the potential energy as a function of temperature for Ga₁₇As₁₃, Ga₃₅As₁₉, Ga₅₅As₄₄ and Ga₈₇As₈₀ nanoparticles.

The C_v is expressed with the relationship between internal energy and temperature;

$$C_v = \left(\frac{\partial E}{\partial T} \right)_v \quad (1)$$

In this study, the internal energy is associated with the interaction potential energy. The calculation of C_v of Ga₁₇As₁₃, Ga₃₅As₁₉, Ga₅₅As₄₄ and Ga₈₇As₈₀ NPs, for the first time, have been investigated using MD to figure out the effect of temperature on C_v . Figure 3 shows temperature dependence of the heat capacity for the Ga₁₇As₁₃, Ga₃₅As₁₉, Ga₅₅As₄₄ and Ga₈₇As₈₀ NPs at different temperatures. For Ga₁₇As₁₃ and Ga₃₅As₁₉, C_v with temperature does not indicate a sharp increase up to about 200 K. After that, it shows a sharp increase as based on temperature increase, however; for Ga₅₅As₄₄ and Ga₈₇As₈₀ NPs, C_v with temperature does not indicate a sharp increase up to about 300 K. After the 300 K, it indicates a sharp increase. These behaviors could be explained with the position and proportion of the core and surface atoms because the surface atoms have lower proportion with increasing the size of the NPs. From obtained results, temperature has a strongly effect on C_v . Moreover, it is interesting to note that the heat capacity behavior of the binary GaAs QDs is found to be in agreement with the previous reported results [25].

The formation of stable structure for some materials is one of the major problems [26] to get high efficiency solar cell devices. Atom distribution in crystalline structures is in general uniform and homogeneous [27]. This behavior at nanoscale may not be conserved, especially under heat treatment [28, 29]. Thus, the order parameter (R_A) is calculated to research the stable structure in NPs by analyzing the distribution of the different types of atoms [30]. R_A is identified by the average distance of a type A atoms in accordance with the center of a NP,

$$R_A = \frac{1}{n_A} \sum_{i=1}^{n_A} r_i \quad (2)$$

where n_A is the number A type atoms in the ternary ABC NPs, and r_i is the distances of the atoms to the coordinate center of the NP. If R_A is a small value, it means that A type atoms are at the center, if R_A is a large value, it means that A type atoms are at the surface region of NP and if R_A is a medium value, it means a well-mixed NP.

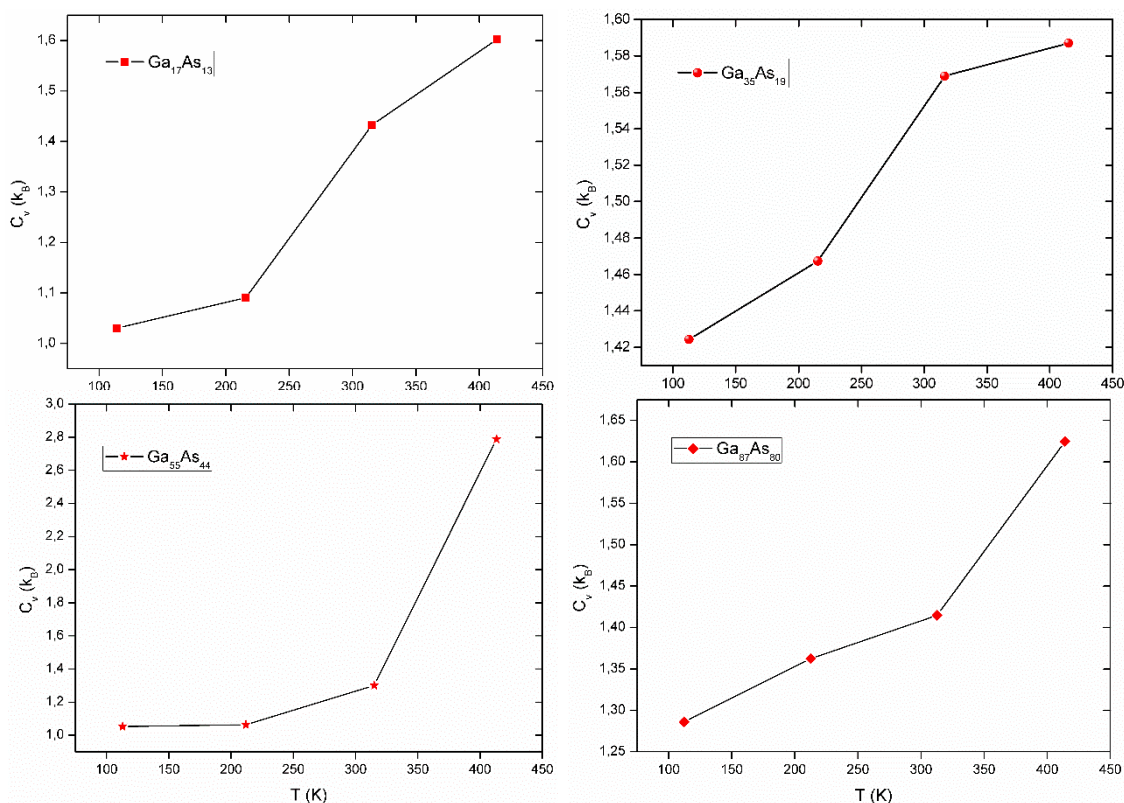


Figure 3. Temperature dependence of the heat capacity for Ga₁₇As₁₃, Ga₃₅As₁₉, Ga₅₅As₄₄ and Ga₈₇As₈₀ nanoparticles at different temperatures.

Figure 4 (a)-(d) shows the behavior of R of Ga and As atoms in accordance with temperature for Ga₁₇As₁₃, Ga₃₅As₁₉, Ga₅₅As₄₄ and Ga₈₇As₈₀ NPs. It is seen that As atoms are on the surface as a general trend. The segregation of As atoms to the surface can be expressed on account of the lower cohesive energy (-2.99 eV) [17] of As atoms and thus they move away from the inner regions of the NPs to the surface regions. Ga atoms are found to be at the center. Ga₈₇As₈₀ has also larger value than that of the other NPs. Depending on the raise of temperature, As atoms show a tendency to the inner regions, however; Ga atoms accumulate at the surface region.

Figure 5 shows coordination number distributions in terms of probability distribution of Ga₁₇As₁₃, Ga₃₅As₁₉, Ga₅₅As₄₄ and Ga₈₇As₈₀ NPs at different temperatures. From Figure 5 probability distribution of all the pair interactions shows different properties based on NP. For example, probability distribution in the Ga₃₅As₁₉ NP decreases with increasing temperature. The distribution of 1-, 2-, 4- and 5-fold coordination is remarkable, the distribution of 3-fold coordination dominates. On the other hand, probability distribution in the Ga₅₅As₄₄ NP increases with increasing temperature. In addition, the distribution of 2-fold coordination dominates.

Figure 6 shows the radial distribution function (RDF) of gallium-gallium (Ga-Ga) and arsenide-arsenide (As-As) interactions of the Ga₃₅As₁₉ nanoparticle at different temperatures. The RDFs is calculated for each atomic pair of optimized Ga₃₅As₁₉ nanoparticle. One can see that As-As has a narrower and higher distribution than Ga-Ga interactions because of the weaker bond [17]. In addition, there is almost no difference in the behavior of RDF between Ga-Ga and As-As atoms. That is, the peak profile in the RDF of Ga-Ga pairs is almost the same when comparing with As-As pairs. The RDF of the peaks for both pairs also decreases based on the temperature increase. Moreover, the fluctuations of obvious peaks in the RDF also increase with raising the temperature. In addition, the peaks of the RDF for the Ga₃₅As₁₉ spherical NP are sharper at 100 K than at 900 K.

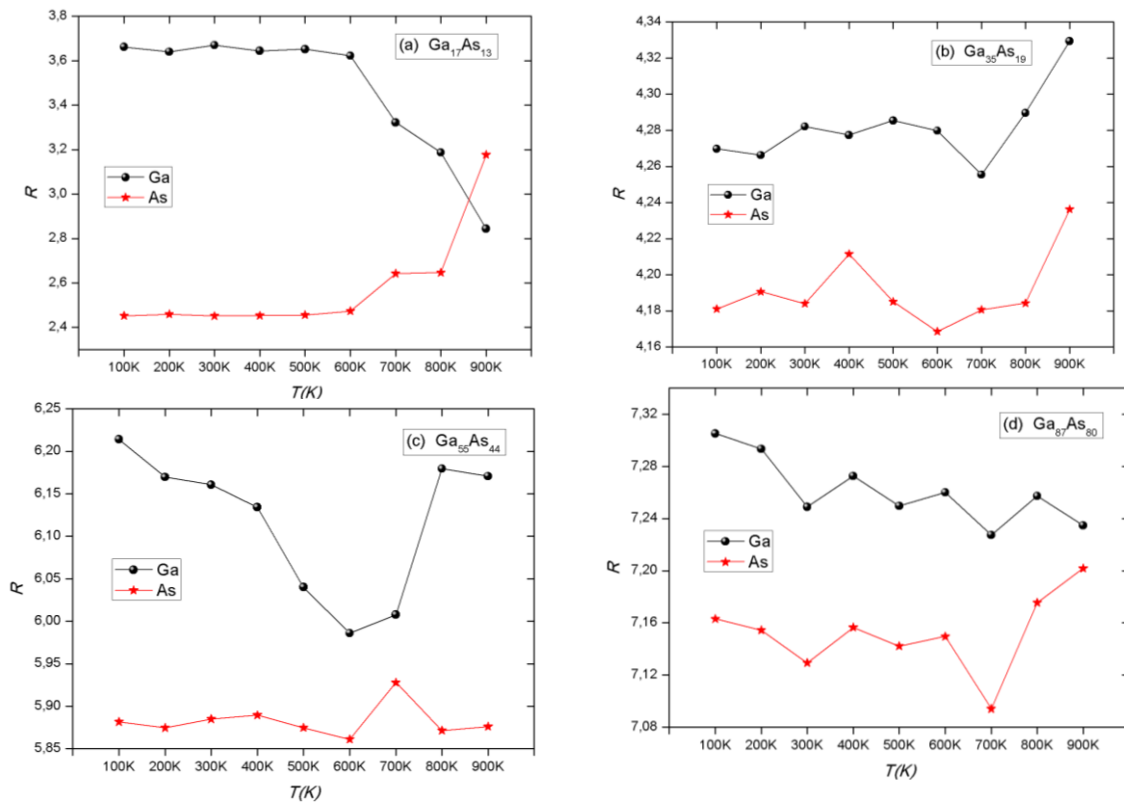


Figure 4. Variation of the order parameter of Ga and As atoms in terms of temperature for (a) Ga₁₇As₁₃, (b) Ga₃₅As₁₉, (c) Ga₅₅As₄₄ and (d) Ga₈₇As₈₀ nanoparticles.

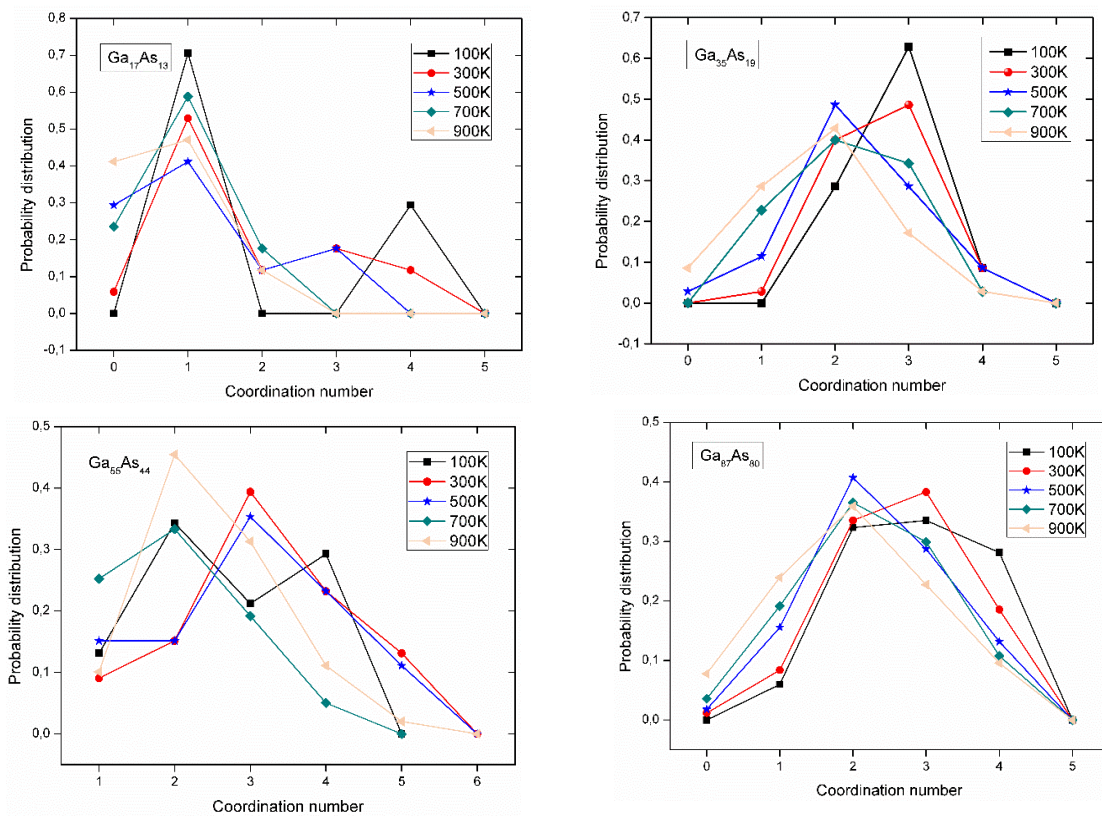


Figure 5. Coordination number distributions of the Ga₁₇As₁₃, Ga₃₅As₁₉, Ga₅₅As₄₄ and Ga₈₇As₈₀ nanoparticles at different temperatures.

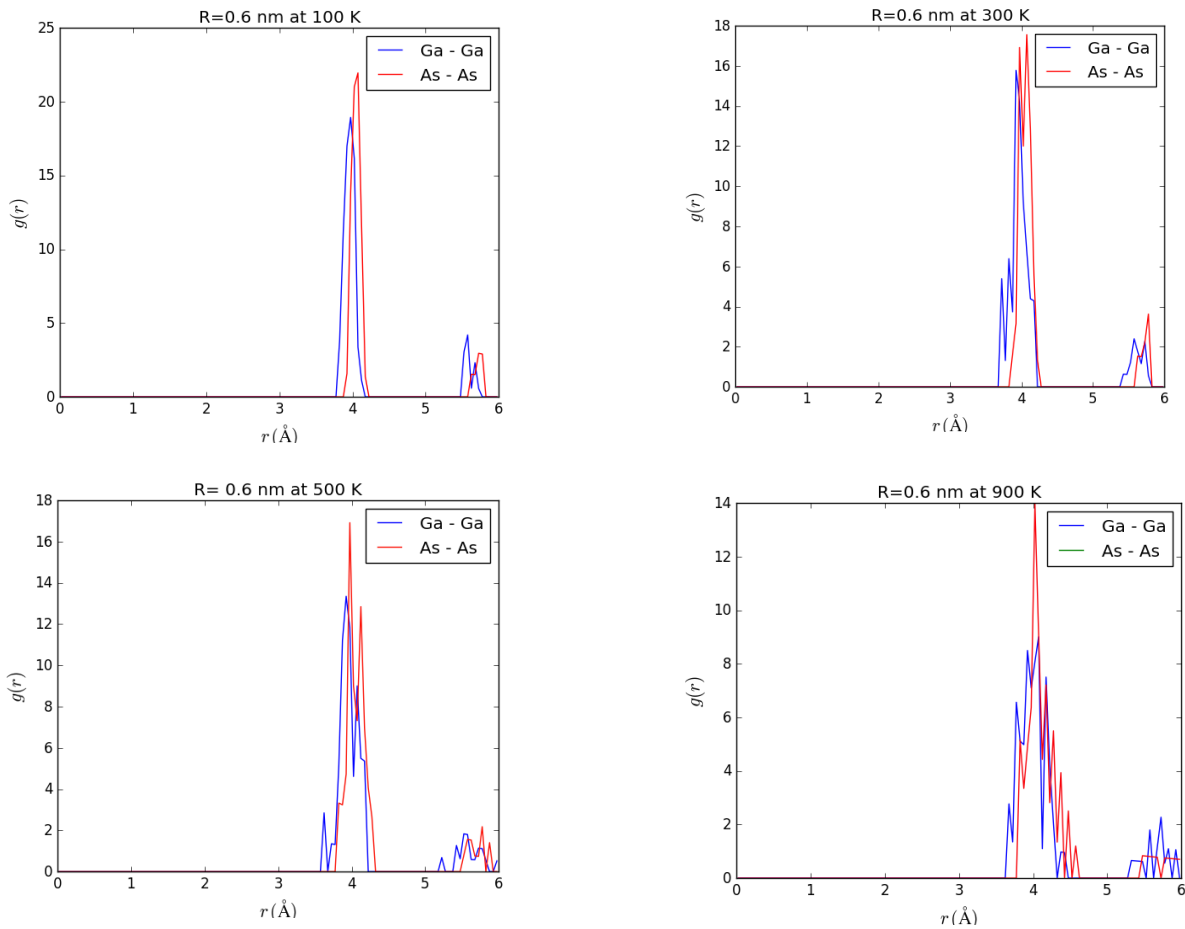


Figure 6. The radial distribution function (RDF) gallium-gallium (Ga-Ga) and arsenide-arsenide (As-As) interactions of the $\text{Ga}_{35}\text{As}_{19}$ nanoparticle at different temperatures.

Figure 7 represents the structures of the of the $\text{Ga}_{35}\text{As}_{19}$ nanoparticle at various temperatures. It is clearly seen that Ga atoms move away from the inner regions of the NP to the surface regions at high temperature (900 K), thus the deformation of the NP increase with increasing temperature.



Figure 7. The structures of the $\text{Ga}_{35}\text{As}_{19}$ nanoparticle at various temperatures.

4. CONCLUSION

I investigated physical properties such as the variation of potential energy depending on temperature and composition, heat capacity (C_v), order parameter (R), coordination number in terms of probability distribution and radial distribution function (RDF) of zinc-blende $\text{Ga}_{17}\text{As}_{13}$, $\text{Ga}_{35}\text{As}_{19}$, $\text{Ga}_{55}\text{As}_{44}$ and $\text{Ga}_{87}\text{As}_{80}$ spherical-like binary NPs by performing MD simulations for the first time. As atoms have significant effect on the stability of GaAs NPs. The tendency of Ga and As atoms inside the core has been observed under temperature increase. The trend of C_v with increasing temperature has been found

to be compatible with available results. Probability distribution of all the pair interactions in the Ga₃₅As₁₉ nanoparticle decreases with increasing temperature. In addition, As-As interactions has a narrower and higher distribution than Ga-Ga pair interactions because of the lower cohesive energy of the As atom.

ACKNOWLEDGEMENTS

This work was supported by the Ahi Evran University Scientific Research Projects Coordination Unit. Project Number: TBY.C1.17.001.

REFERENCES

- [1] Wang CL, Zhang H, Zhang JH, Li MJ, Sun H, Z. Yan B. Application of Ultrasonic Irradiation in Aqueous Synthesis of Highly Fluorescent CdTe/CdS Core-Shell Nanocrystals. *J Phys Chem C* 2007; 111: 2465–2469.
- [2] Yang P, Tretiak S, Masunov AE, Ivanov SJ. Quantum chemistry of the minimal CdSe clusters. *Chem Phys* 2008; 129(7): 74709-1-74709–12.
- [3] Kushwaha AK. Lattice dynamical calculations for HgTe, CdTe and their ternary alloy CdxHg1-xTe. *Comput Mater Sci* 2012; 65: 315–319.
- [4] Streetman BG, Sanjay B. *Solid State Electronic Devices*. 5th ed. Prentice Hall, New Jersey, 2000.
- [5] Pluengphon P, Bovornratanaraks T, Vannarat S, Pinsook U. Structural and mechanical properties of GaAs under pressure up to 200 Gpa. *Solid State Commun* 2014; 195: 26-30.
- [6] Smida A, Laatar F, Hassen M, Ezzaouia H. Structural and optical properties of vapor-etched porous GaAs. *J Lumin* 2016; 176: 118–123.
- [7] Saghrouni H, Jomni S, Cherif A, Belgacem W, Beji L. The temperature dependence on the electrical properties of dysprosium oxide deposited on n-porous GaAs. *J Alloys Compd* 2016; 676: 127-134.
- [8] Danilchenko BA, Budnyk AP, Shpinar LI, Yaskovets II, Barnham KWJ, Ekins-Daukes N. Radiation resistance of GaAs solar cells and hot carriers. *J Sol Energy Mater Sol Cells* 2011; 95: 2551–2556.
- [9] Yoon J, Jo S, Chun IS, Jung I, Kim H-S, Meitl M, Menard E, Li X, Coleman JJ, Paik U, Rogers JA. GaAs photovoltaics and optoelectronics using releasable multilayer epitaxial assemblies. *Nat Lett* 2010; 465: 329-333.
- [10] Moon S, Kim K, Kim Y, Heo J, Lee J. Highly efficient single-junction GaAs thin-film solar cell on flexible substrate. *Sci Rep* 2016; 6: 30107-1- 30107-6.
- [11] Li Q, Shen K, Yang R, Zhao Y, Lu S, Wang R, Dong J, Wang D. Comparative study of GaAs and CdTe solar cell performance under low-intensity light irradiance. *Sol Energy* 2017; 157: 216-226.
- [12] Brus L. Electronic wave functions in semiconductor clusters: experiment and theory. *J Phys Chem* 1986; 90 (12): 2555–2560.
- [13] Graf A, Sonnenberg D, Paulava V, Schliwa A, Heyn Ch, Hansen W. Excitonic states in GaAs quantum dots fabricated by local droplet etching. *Phys Rev B* 2014; 89: 115314-1-115314-6.

- [14] Sallen G, Kunz S, Amand T, Bouet L, Kuroda T, Mano T, Paget D, Krebs O, Marie X, Sakoda K, Urbaszek B. Nuclear magnetization in gallium arsenide quantum dots at zero magnetic field. *Nat Commun* 2014; 5: 3268-1-3268-7.
- [15] LAMMPS, lammps.sandia.gov/download.
- [16] Plimpton S. Fast Parallel Algorithms for Short-Range Molecular Dynamics. *Comput Phys* 1995; 117: 1-19.
- [17] Murdick DA, Zhou XW, Wadley HNG, Nguyen-Manh D, Drautz R, Pettifor DG. Analytic bond-order potential for the gallium arsenide system. *Phys Rev B* 2006; 73: 045206-1-045206-20.
- [18] Ward DK, Zhou XW, Wong BM, Doty FP, Zimmerman JA. Accuracy of existing atomic potentials for the CdTe semiconductor compound. *J Chem Phys* 2011; 134: 244703-1-244703-13.
- [19] Ward DK, Zhou XW, Wong BM, Doty FP, Zimmerman JA. Analytical bond-order potential for the cadmium telluride binary system. *Phys Rev B* 2012; 85: 115206-1-115206-19.
- [20] Zhou XW, Ward DK, Wong BM, Doty FP. Melt-Growth Dynamics in CdTe Crystals. *Phys Rev Lett* 2012; 108: 245503-1-245503-4.
- [21] Nosé S. A unified formulation of the constant temperature molecular dynamics methods. *J Chem Phys* 1984; 81: 511-519.
- [22] Hoover WG. Canonical dynamics: Equilibrium phase-space distributions. *Phys Rev* 1985; A31: 1695-1697.
- [23] Humphrey W, Dalke A, Schulten, K. VMD - Visual Molecular Dynamics. *J Molec Graphics* 1996; 14: 33-38.
- [24] Hanha TTT, Hoang VV. Structure and diffusion in simulated liquid GaAs. *Eur Phys J Appl Phys* 2010; 49: 30301-p1-30301-p7.
- [25] Boyacioglu B, Chatterjee A. Heat capacity and entropy of a GaAs quantum dot with Gaussian confinement. *J Appl Phys* 2012; 112: 083514-1-083514-6.
- [26] Yu T-C, Brebrick RF. The Hg-Cd-Zn-Te phase diagram. *J Phase Equilib* 1992; 13: 476-496.
- [27] Lu C, Cheng Y, Pan Q, Tao X, Yang B, Ye G. One-dimensional Growth of Zinc Crystals on a Liquid Surface. *Sci Rep* 2016; 6: 19870-1-19870-7.
- [28] Kurban M, Malcioğlu OB, Erkoç Ş. Structural and thermal properties of Cd-Zn-Te ternary nanoparticles: Molecular-dynamics simulations. *Chem Phys* 2016; 464: 40-45.
- [29] Kurban M, Erkoç Ş. Segregation formation, thermal and electronic properties of ternary cubic CdZnTe clusters: MD simulations and DFT calculations. *Physica E* 2017; 88: 243-251.
- [30] Wu X, Wei Z, Liu Q, Pang T, Wu G. Structure and bonding in quaternary Ag-Au-Pd-Pt clusters. *J Alloys Compd* 2016; 687: 115-120.